Available online at www.sciencedirect.com
SCIENCE DIRECT®
Neuroscience Research 48 (2004) 155–167
Neuroscience Research
www.elsevier.com/locate/neures

Architecture of binocular disparity processing in monkey inferior temporal cortex

Kenji Yoshiyama [a], Takanori Uka [b], Hiroki Tanaka [b,c], Ichiro Fujita [a,b,c,*]

[a] *Department of Cognitive Neuroscience, Osaka University Medical School, Yamadaoka 2-2, Suita, Osaka 565-0871, Japan*
[b] *Core Research for Evolutional Science and Technology, Japan Science and Technology Corporation, Japan*
[c] *Graduate School of Frontier Biosciences and Graduate School of Engineering Science, Osaka University, Machikaneyama 1-3, Toyonaka, Osaka 560-8531, Japan*

Received 2 September 2003; accepted 24 October 2003

Abstract

Neurons in the inferior temporal (IT) cortex respond not only to the shape, color or texture of objects, but to the horizontal positional disparity of visual features in the right and left retinal images. IT neurons with similar shape selectivity cluster in columns. In this study, we examined how IT neurons are spatially arranged in the IT according to their selectivity for binocular disparity. With a single electrode, we simultaneously recorded extracellular action potentials from a single neuron and those from background multiple neurons at the same sites or recorded multineuronal responses at successive sites along electrode penetrations, while monkeys performed a fixation task. For neurons at each recording site, effective shapes were first determined from a set of 20 shapes presented at the zero-disparity plane. The most effective shape was then presented with varying amounts of disparity. Single neuron responses and background multiunit responses recorded at the same sites showed a similar ability of disparity discrimination and tended to share the preferred disparity, suggesting that neurons with similar disparity selectivity are clustered in the IT. We estimated from sequential recordings along electrode penetrations that the size of the neuronal clusters with similar disparity selectivity was smaller than the size of clusters with similar shape selectivity.

Keywords: Horizontal binocular disparity; Ventral visual pathway; Area TE; Macaque; Shape

1. Introduction

Horizontal binocular disparity provides an important visual cue for the perception of depth and three-dimensional (3-D) scenes (Wheatstone, 1838). In the primate visual cortex, neurons selective for binocular disparity are found already in the first and lower cortical stages, V1, V2, and V3. In higher cortical processing stages, these neurons are found along the "dorsal" pathway, including the middle temporal area (MT), the medial superior temporal area and the posterior parietal cortex, and also along the "ventral" pathway in area V4 and the inferior temporal (IT) cortex (Hubel and Wiesel, 1970; Poggio and Fischer, 1977; Maunsell and Van Essen, 1983; Burkhalter and Van Essen, 1986; Felleman and Van Essen, 1987; Hubel and Livingstone, 1987; Poggio et al., 1988; Roy et al., 1992; Eifuku and Wurtz, 1999; Taira et al., 2000; Uka et al., 2000; Hinkle and Connor, 2001; Watanabe et al., 2002). In both area V4 and the IT, most disparity-selective neurons show position invariance of their disparity selectivity (Uka et al., 2000; Watanabe et al., 2002). The disparity preference of most disparity-selective IT neurons does not change depending on the stimulus shape (Uka et al., 2000). In addition to neurons sensitive to position-in-depth, area V4 contains neurons selective for bars oriented in depth (Hinkle and Connor, 2002), and the IT contains both neurons selective for particular 3-D surfaces defined by disparity gradients and curvature (Janssen et al., 2000, 2001) and neurons selective for the shape of surfaces defined solely by disparity (Tanaka et al., 2001).

The degree of disparity tuning and the preferred range of disparity differ among neurons within each of the above-mentioned areas. Previous studies suggest that disparity-selective neurons are clustered according to these tuning properties. In cat and monkey V1, neurons show weak clustering based on disparity selectivity (Blakemore,

* Corresponding author. Tel.: +81-6-6850-6510; fax: +81-6-6857-5421.
E-mail address: fujita@fbs.osaka-u.ac.jp (I. Fujita).

0168-0102/$ – see front matter
doi:10.1016/j.neures.2003.10.008

1970; LeVay and Voigt, 1988; Prince et al., 2002). In V2, disparity-selective neurons are found more abundantly in the thick cytochrome oxidase (CO) stripes than in the thin and pale stripes (Hubel and Livingstone, 1987; Peterhans and von der Heydt, 1993; Roe and Ts'o, 1995). It has been suggested that clustering of disparity-selective neurons in the thick stripes takes a columnar form (Roe and Ts'o, 1995; Ts'o et al., 2001). Area V3 is reported to consist of columns of neurons selective for similar disparities (Adams and Zeki, 2001). The most compelling evidence for columnar clustering of disparity-selective neurons comes from MT where neurons with similar sensitivity to disparity and preferred range of disparity are arrayed vertically across the cortical layers, and the preferred disparity gradually shifts in tangential direction across the cortical surface (DeAngelis and Newsome, 1999).

We have previously demonstrated that V4 neurons are clustered according to disparity discrimination ability and preferred disparity (Watanabe et al., 2002). Less is known about the spatial organization of disparity-selective neurons in the IT, except for evidence that disparity tuning curves are correlated between nearby IT neurons (Uka et al., 2000). In this study, we extended this previous finding by quantitatively comparing the disparity tuning curves, the ability of disparity discrimination, and the preferred range of disparity between a single neuron and its nearby multiple neurons in the IT. We also estimated the size of clusters of disparity-selective neurons by recording multi-neuronal responses at 0.2 mm intervals along electrode penetrations. Parts of these results have been previously reported in abstract form (Yoshiyama et al., 2000).

2. Materials and methods

The general procedures for surgery and animal care have been previously described in detail (Uka et al., 2000). All animal care and experimental procedures were performed in accordance with the NIH Guide for the Care and Use of Laboratory Animals and were approved by the animal experiment committee of Osaka University. Extracellular action potentials ("spikes") were recorded from single neurons or a small group of neurons in the IT of five hemispheres in three male Japanese monkeys *(Macaca fuscata*, 6–7 kg bw; Fig. 1). Most of the data were obtained from monkeys 1 and 2. We made additional recordings in monkey 3, one of the subjects in a previous study (Uka et al., 2000), to analyze the degree of clustering of disparity-selective neurons using different sets of shape stimuli.

2.1. Surgery

Using standard aseptic surgical procedures and pentobarbital sodium anesthesia (35 mg/kg i.p.), we attached a head holder to the skull of each monkey to fix its head to a monkey chair. Search coils were implanted under the conjunctiva of both eyes to monitor eye positions (Judge et al., 1980) as previously described (Uka et al., 2000). Recording chambers were attached to the temporal part of the skull. After the surgery, the monkeys were treated with an antibiotic (piperacillin sodium, 30 mg/kg i.m.), an analgesic (ketoprofen, 0.5 mg/kg i.m.), and a corticosteroid (dexamethasone sodium phosphate, 0.1 mg/kg i.m.) to reduce potential inflammation.

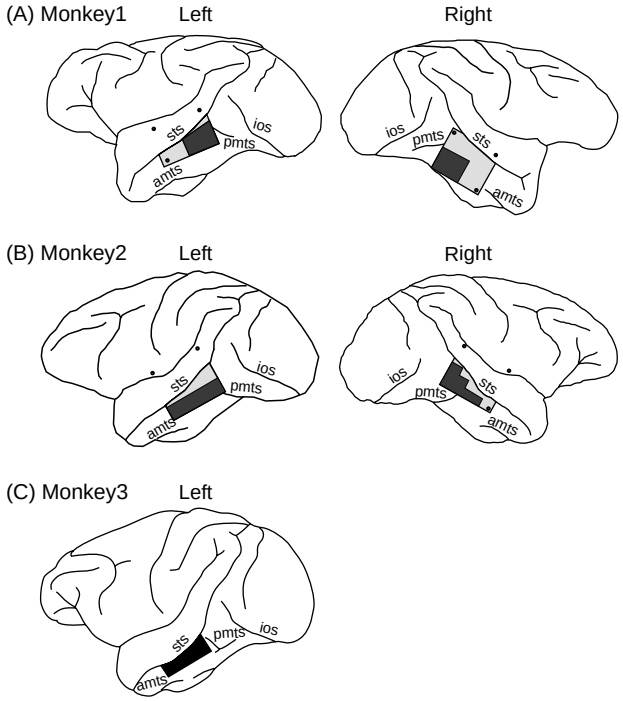

Fig. 1. The recording regions (shaded area) in five cerebral hemispheres of three monkeys: (A) monkey 1; (B) monkey 2; (C) monkey 3. The regions contained areas TEd, TEOd, TEOv, and the ventral bank of the superior temporal sulcus. Most recordings were made in blackened regions. The dots in each hemisphere indicate the location of the pins implanted at the corners of the recording chamber.

2.2. Task and stimuli

Monkeys sitting on a chair faced a 17-inch color monitor (RD17GR, Mitsubishi, Tokyo) placed 57 cm away. The monkeys were trained for a computer-controlled fixation task. The positions of both eyes were sampled at a rate of 100 Hz using a search coil technique. A gray spot ($0.2^\circ \times 0.2^\circ$) was presented at the center of the monitor on a black background (luminance 1.0 cd/m^2). The monkeys were required to fixate within a $2.0^\circ \times 2.0^\circ$ electronic (invisible) window centered on the spot within 500 ms. After an additional 500 ms, a stimulus appeared on the monitor. In order to avoid eliciting vergence eye movement, stimuli were presented 2° horizontally away from the fixation spot and contralaterally to the recording hemisphere. Stimuli were 3° or less across and did not overlap the fixation point. The monkeys had to maintain their fixation within the fixation window throughout the 1 s period of visual stimulus presentation in order to

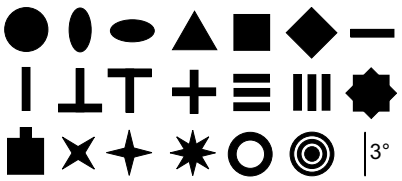

Fig. 2. The stimulus set for testing response selectivity for shape. In the experiments, stimuli were shown in red on the black screen.

receive a drop of water. The task was immediately aborted if they broke their fixation.

For neurons recorded at each site, the shape that evoked the strongest response was selected from 20 geometric shapes (Fig. 2). Each stimulus was presented five times in random order at the zero-disparity plane. Red color (luminance 5.7 cd/m^2) was used for shapes, because red phosphors are short-lived compared to the other colors, making it possible to obtain better stereo separation between the two eyes. Binocular disparities of various amounts were then added to the most effective shape. Disparity varied from -0.8° (crossed or "near" disparity) to 0.8° (uncrossed or "far" disparity) at 0.2° intervals. The stimuli at each disparity were presented 10 times in random order. Stereoscopic stimulation was achieved using a liquid-crystal stereoscopic modulator (SGS610, Tektronix, Beaverton, Oregon, refresh rate: 70 Hz for each eye).

After each session, the monkeys were returned to their cages. The water supply was restricted in the home cages. Food was made available to the monkeys ad libitum.

2.3. Electrophysiological recordings

A 3 mm hole was made in the skull within the recording chamber 1 day before we started recording. A tungsten microelectrode (impedance 1–2 MΩ at 1 kHz; Frederic Haer Company, Bowdoinham, ME) was advanced from the lateral side of the skull with a micromanipulator (MO-95s, Narishige, Tokyo) mounted on an adapter attached to the recording chamber. The electrode penetrated the dura mater to reach the lateral surface of the IT. Extracellular spikes from small groups of neurons were recorded at 0.2 mm intervals from the brain surface to the white matter using a conventional amplifier and a window discriminator. Whenever possible, we isolated single unit (SU) activity from the background multi unit (MU) activity using another window discriminator. We placed a gap between the lower threshold of the first window for isolating SU spikes and the upper limit of the second window for MU spikes, so that SU spikes did not fall into the second window. We also continuously monitored the spike forms of SU and MU so as not to erroneously assign the second, smaller peak of triphasic action potentials from SU to the second channel for MU responses. The number of spikes recorded during the task was counted using a computer. In some penetrations, we made electrolytic lesions by passing an electric current of 10 μA for 50 s after the recording session to identify the trajectory of the penetration in later histological analysis.

2.4. Histology

After all of the experiments were completed, we implanted four pins into the brain at each corner of the recording chamber under anesthesia with pentobarbital sodium (Fig. 1). The animals were then given an overdose of pentobarbital sodium (60 mg/kg i.p.), the chest cavity was opened, and heparin (200 IU/kg) was injected into the heart. The animals were transcardially perfused with 500 ml of phosphate-buffered saline (PBS, pH 7.4, 37 °C) and with a fixative solution consisting of 1000 ml of ice-cold 4% paraformaldyhyde, 0.1% glutaraldehyde in 0.1 M PBS, and further with 800 ml of ice-cold 4% paraformaldehyde in 0.1 M PBS. The brain was removed, photographed, blocked, post-fixed overnight in 4% paraformaldehyde in 0.1 M PBS, and soaked in 0.1 M PBS containing a graded series of sucrose (10–30%). The location of the implanted electrodes was verified for reconstruction of the recording area. Serial frozen sections were cut coronally or in parallel with the edge of the recording chamber at 100 μm thickness. All sections were stained for Nissl substance with cresyl violet.

2.5. Data analysis

The ongoing firing rate in the absence of stimulus ("spontaneous" firing rate) was calculated during the 500 ms period immediately prior to stimulus presentation, while the monkey gazed at the fixation point. The response magnitude was calculated from the firing rate during a 1 s period starting 80 ms after the onset of the stimulus. Both were calculated for each trial, the spontaneous firing rate was averaged over all trials, and the magnitude of the responses to the stimulus was averaged over five trials for each shape stimulus or 10 trials for each disparity. All statistical analyses were performed using the magnitude of responses to the stimulus. We conducted an ANOVA test to examine whether the average vergence angle differed among the trials tested with the nine different disparities. The neuronal data were discarded when the vergence angle changed across different disparity stimuli ($P < 0.05$), in order to ensure that the stimulus disparity on the screen corresponded to the disparity of their retinal projections.

Disparity selectivity was quantified by calculating the disparity-discrimination index (DDI; Prince et al., 2002; DeAngelis and Uka, 2003). The index was defined as

$$\mathrm{DDI} = \frac{R_{\max} - R_{\min}}{R_{\max} - R_{\min} + 2\sqrt{\mathrm{SSE}/(N-M)}}$$

where $R_{\max}$ and $R_{\min}$ denote the maximum and the minimum magnitudes of response elicited by stimuli with various amounts of disparity, SSE is the summed squared error around the mean response across all disparities, N is the number of trials, and M is the number of stimulus

conditions tested. All of these calculations were performed using the square-root counts of the firings, because the variability of neuronal firing across trials increases with the mean firing rate and the residual variance will be biased toward the larger values produced by firing rate. The square-root transformation of the spike counts substantially decreases this bias (Prince et al., 2002).

3. Results

3.1. Recording site

Our recording chambers covered the posterolateral part of the inferior temporal cortex straddling or anterior to the posterior middle temporal sulcus (pmts) (shaded areas in Fig. 1). Within this area, recordings were made mostly from the posterior part of area TEd, and partly from area TEOd, the ventral bank of the superior temporal sulcus (sts), and the posterior part of area TEv (blackened areas). Because we did not observe obvious differences among the areas, we have combined the data and will describe them together.

3.2. Disparity selectivity of adjacent neurons recorded with a single electrode

We recorded at a total of 469 sites in the IT (158 in monkey 1; 288 in monkey 2; 23 in monkey 3). At 93 of these sites (26 in monkey 1; 50 in monkey 2; 17 in monkey 3), we separated SU activity from concurrently recorded MU activity, and both types of activity showed statistically significant visual responses to one or more of the 20 shapes in the initial test (Wilcoxon's signed rank test, $P < 0.05$). At 47 of the 93 recording sites (51%), both SU and MU activity changed depending on disparity (Kruskal–Wallis test, $P < 0.05$). At 15 sites (16%), only SU responses were disparity selective, and at another 11 sites (12%), only MU responses were selective. At the remaining 20 sites (22%), neither SU nor MU responses changed with disparity (Kruskal–Wallis test, $P > 0.05$). Thus, disparity-selective SUs tended to be found with disparity-selective MUs, and non-selective SUs tended to be recorded with non-selective MUs (χ^2-test, $P < 0.001$).

Fig. 3 shows the disparity–tuning curves of pairs of simultaneously recorded SU and MU responses at four illustrative sites. Fig. 3A shows an example of a recording site where the tuning curves of both SU and MU had a well-defined peak at zero disparity ("tuned-0" type of Poggio et al., 1988). Fig. 3B is an example of a recording site where SU and MU responded more strongly to crossed disparities than to uncrossed disparities, showing a "near-cell" type of tuning. Fig. 3C is an example of SU and MU tuning curves of a "far-cell type", which showed larger responses at uncrossed disparities than at crossed disparities. In all of these cases, the mean responses to different disparities were highly correlated between SU and MU (Pearson's correlation coefficient $r = 0.87$ for A, 0.82 for B, 0.97 for C; $P < 0.05$; hereafter referred to as "disparity correlation coefficient"). Fig. 3D shows an example of a site where neither the SU nor MU responses changed with disparity (Kruskal–Wallis test, $P > 0.05$). These examples show that neurons recorded at the same sites (i.e., neighboring neurons) often had similar disparity tuning curves.

For population analysis we first focused on the neuronal pairs at the 73 ($47 + 15 + 11$) sites where both SU and MU showed statistically significant visual responses (Wilcoxon's signed rank test, $P < 0.05$), and SU or MU or both were selective for disparity (Kruskal–Wallis test, $P < 0.05$). We calculated disparity correlation coefficients for comparison with the results in our previous study (Uka et al., 2000). The distribution of disparity correlation coefficients between pairs of SU and MU at the same sites was highly skewed toward positive values (Fig. 4A; median 0.73, $n = 73$). The correlation was statistically significant in 42 of the 73 pairs (55%, $P < 0.05$; shaded columns). All but 2 of the 42 cell pairs showed a positive correlation. On the other hand, the distribution of correlation between unit pairs recorded at different sites was centered at 0 (median -0.01, $n = 5256$; Fig. 4B). Approximately equal numbers of statistically significant correlations were observed for negative and positive directions. The two distributions in Fig. 4A and B were statistically different (Mann–Whitney U-test, $P < 0.0001$).

The high correlation of disparity tuning for simultaneously recorded pairs was not due to contamination between SU recordings and background MU recordings. During recording sessions, we monitored spike forms in the two recording channels to ensure the absence of cross-talk between them. As a further test, we subtracted the SU spike counts from the MU spike counts. Even if all of the SU spikes had fallen into the MU channel, this procedure would eliminate the effect of contamination. Even after this procedure, the correlation coefficients between the SU responses and the subtracted MU responses were biased towards positive (Fig. 4C, median 0.45), and were significantly different from the distribution of the units recorded at different sites shown in Fig. 4B (Mann–Whitney U-test, $P < 0.0005$). These results indicate that nearby IT neurons show a strong tendency to have similar disparity tuning curves, although a few sites showed clearly negative SU–MU correlation.

The median (0.73) of the disparity correlation coefficients between SU and MU responses was substantially higher than the one we obtained in our previous study (0.30; Uka et al., 2000). This difference was not due to the difference in the nature of recordings (i.e., both SU–SU and SU–MU pairs were analyzed in the previous study and only SU–MU pairs were analyzed in the present study), because we previously showed that the distribution of the disparity correlation coefficients is similar between SU–SU pairs and SU–MU pairs (Fig. 13 of Uka et al., 2000). One possible reason for this difference may be the difference in the shape-preference test between the two studies. The initial stimulus set in the previous study consisted of 11 simple geometric shapes including four

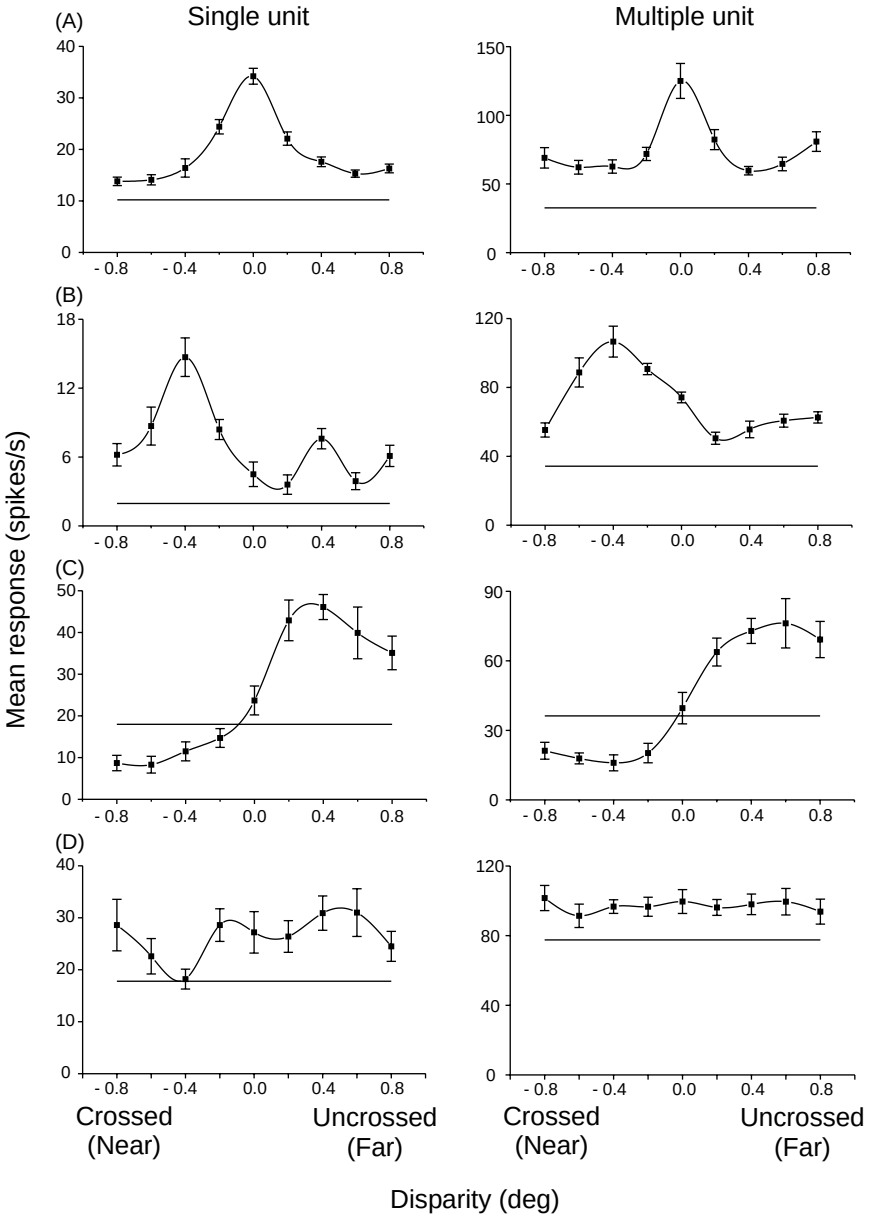

Fig. 3. Comparison of disparity selectivity between pairs of simultaneously recorded single unit (SU) and multiunit (MU) activity. Examples of four representative sites are shown. Each data point shows the mean response across 10 stimulus repetitions, and error bars indicate the standard error of the mean. Data points were fitted by spline interpolation. The horizontal lines show the spontaneous firing rates. (A) Responses at a "tuned-excitatory cell" site. The disparity correlation coefficient $r = 0.87$; the disparity discrimination index (DDI) = 0.71 (SU) or 0.59 (MU); the preferred disparity (PD) = −0.01 (SU) or 0.01 (MU). (B) Responses at a "near-cell" site. $r = 0.82$; DDI = 0.58 (SU) or 0.64 (MU); PD = −0.41 (SU) or −0.41 (MU). (C) Responses at a "far-cell" site. $r = 0.97$; DDI = 0.64 (SU) or 0.63 (MU); PD = 0.33 (SU) or 0.60 (MU). (D) Responses at a "non-selective cell" site. $r = 0.55$; DDI = 0.38 (SU) or 0.21 (MU).

bars, two crosses, a circle, an oval, and a star, while the stimulus set in this study consisted of 20 shapes (Fig. 2). This set was richer, which may increase the likelihood that it contains stimuli that activate individual IT neurons more strongly. This may, in turn, allow a reliable assessment of disparity selectivity and result in a higher disparity correlation coefficient between simultaneously recorded neurons. The maximum firing rate during stimulus presentation was indeed statistically higher for the disparity-selective SUs tested with the present stimulus set (18.7 ± 13.3 spikes/s, mean ± S.D., $n = 62$) than those tested with the previous stimulus set (8.8 ± 10.1 spikes/s, $n = 24$, Mann–Whitney U-test, $P < 0.0001$). We then tested IT neurons in the monkey that was used in the previous study (monkey 3) with our current stimulus set, determined the best shape out of the 20 stimuli, and compared the disparity selectivity between simultaneously recorded neurons. The median of the disparity correlation coefficient between the neuronal pairs was 0.76 ($n = 17$,

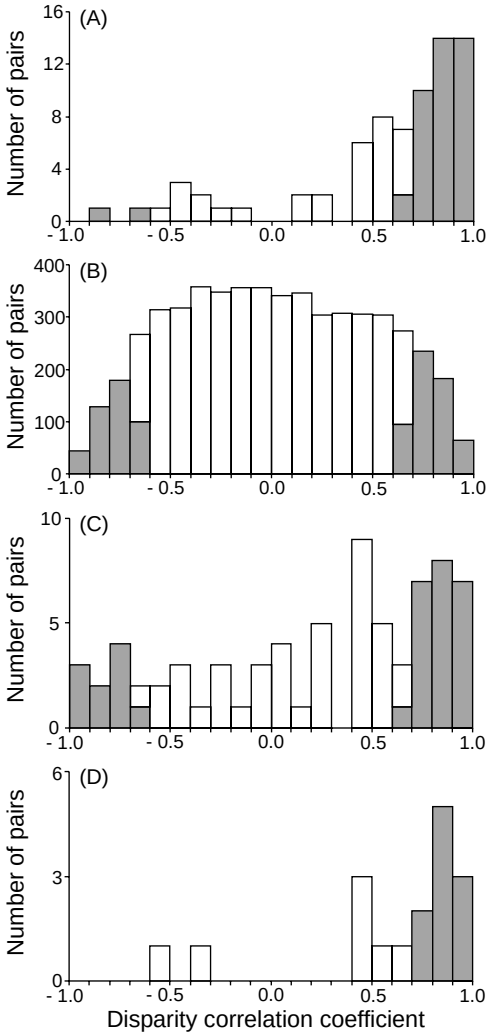

Fig. 4. The frequency distribution of disparity correlation coefficients. (A) The disparity correlation coefficients for pairs of SU and MU responses recorded at the same site. Data were obtained from sites where at least one of the units was selective for disparity. The distribution was shifted toward positive values (median = 0.73). Filled bars indicate the pairs with statistically significantly correlations ($r > 0.67$, $P < 0.05$) in this and the other three histograms. (B) The disparity correlation coefficients for pairs of SU and MU responses recorded from different sites. The distribution was centered near 0 (median = −0.01). (C) The disparity correlation coefficients for pairs of SU responses and the spike count of MU responses minus the SU responses at the same site. The distribution was still shifted toward positive (median = 0.45) after the subtraction. (D) The disparity correlation coefficients for pairs of SU and MU responses from monkey 3. Median = 0.76.

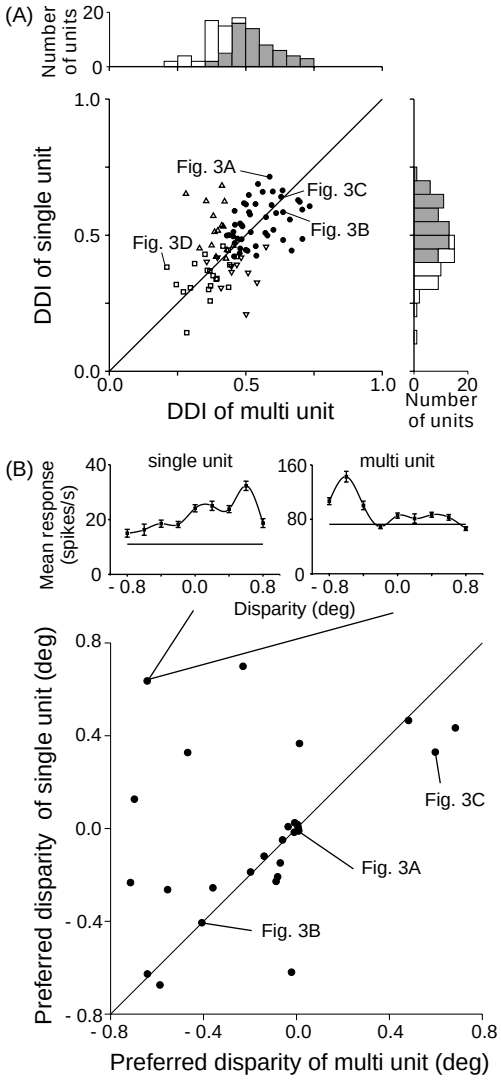

Fig. 5. Quantitative comparison of the disparity discrimination index (DDI) and the preferred disparity between simultaneously recorded SU and MU responses. In each panel, data from SUs are plotted on the ordinate and data from MUs on the abscissa. The solid diagonal lines are the identity lines. (A) DDIs. Circles: both the SU and MU are disparity selective. Inverse triangles: only the SU is disparity selective. Triangles: only the MU is disparity selective. squares; neither the SU nor MU is disparity selective. Histograms at the top and right show the distributions of DDI of MUs and SUs, respectively. Filled bars indicate disparity-selective units. (B) Preferred disparities. Upper disparity–tuning curves were recorded at the site where the preferred disparity was the most different between SU and MU.

Fig. 4D); no difference was found in the coefficient values among the three monkeys ($n = 26$ for monkey 1, $n = 50$ for monkey 2; Kruskal–Wallis test, $P = 0.58$). These results indicate that the difference between the present results and the previous results (Uka et al., 2000) was mostly due to the difference in the initial stimulus set rather than an intersubject difference in the organization of disparity sensitive neurons.

We next compared the abilities of nearby neurons to signal different disparities. Fig. 5A plots the disparity-discrimination index (DDI) for SU against the DDI for all 93 simultaneously recorded MU. Data points were distributed in an elliptical region along the diagonal line, indicating that the DDI of SU correlated with the DDI of MU recorded at the same site ($n = 93$, Pearson's correlation $r = 0.53$; $P < 0.0001$). The four examples discussed in Fig. 3A–D are labeled as such in Fig. 5A. The results indicate that nearby neurons have similar abilities to discriminate disparities. Disparity selectivity assessed with the Kruskal–Wallis test agreed well with the distribution of DDIs; DDIs for

disparity-selective SU and MU (filled circles) were higher ($n = 47$) than DDIs for the sites where either SU or MU was disparity selective (triangles and inverse trinagles; $n = 26$), and DDIs of the latter group were in turn higher than DDIs for the sites where neither SU nor MU was disparity selective (squares; $n = 20$). Note, however, that the DDIs of both SU and MU responses showed single-peak distributions (histograms shown upper and right in Fig. 5A). Disparity-selective and non-selective neurons did not form distinct groups, but rather belonged to a spectrum of neurons with various degrees of disparity selectivity. DDIs of SU and MU were 0.48 ± 0.12 and 0.47 ± 0.11 (mean $\pm$ S.D., $n = 93$); there was no difference between these groups (Mann–Whitney U-test, $P = 0.72$). The spontaneous firing rate of MU was on average 7.8 times higher than that of SU in our sample, suggesting that our MU recordings contain approximately 8 neurons. The similar DDIs for SU and MU (i.e., failure to improve DDIs by combining activity from multiple adjacent neurons) suggest that disparity selectivity was not perfectly identical among nearby neurons.

Fig. 5B compares the preferred disparity determined from the spline-fitted tuning curves for pairs of simultaneously recorded SU and MU. Data are plotted for a subset of recordings (28 of the 47 disparity-selective sites) where the response peaks of both SU and MU were within the examined range of disparity (less than $\pm 0.8^\circ$). Data points tended to be distributed along the diagonal line with several notable exceptions where points were off the line (Pearson's correlation coefficient $r = 0.38$; $P < 0.05$). The three examples discussed in Fig. 3A–C are indicated as such in Fig. 5B. The SU–MU pair with the most discrepant preferred disparity lies at the left-upper corner of the scatter plot, and is shown with its disparity tuning curves. The SU most preferred the uncrossed disparity of 0.6°, while the MU preferred the crossed disparity of 0.6°. The disparity correlation coefficient for this SU–MU pair was -0.40. The results in Figs. 3–5 indicate that neurons with similar disparity–tuning properties tended to be spatially clustered in the IT.

If the high correlation of responses between simultaneously recorded SU and MU resulted from factors other than disparity selectivity (e.g., attentional effects), the correlation values would be independent of disparity selectivity of SU and MU. We therefore analyzed the relationship between disparity correlation coefficients and DDIs by making scatter plots of the two values (Fig. 6). Disparity correlation coefficients between SU and MU were only weakly correlated with DDIs of MU ($r = 0.20$, $n = 93$, $P < 0.05$), or the correlation fell a little short of statistical significance with DDIs of SU ($r = 0.17$, $n = 93$, $P = 0.057$). However, this low correlation was due to the eight recording sites where SU and MU showed discrepant tuning curves and hence low SU–MU correlations (filled circles at lower right corner in Fig. 6A and B). The other data points showed a clear trend that the higher the DDIs, the higher the disparity correlation coefficients.

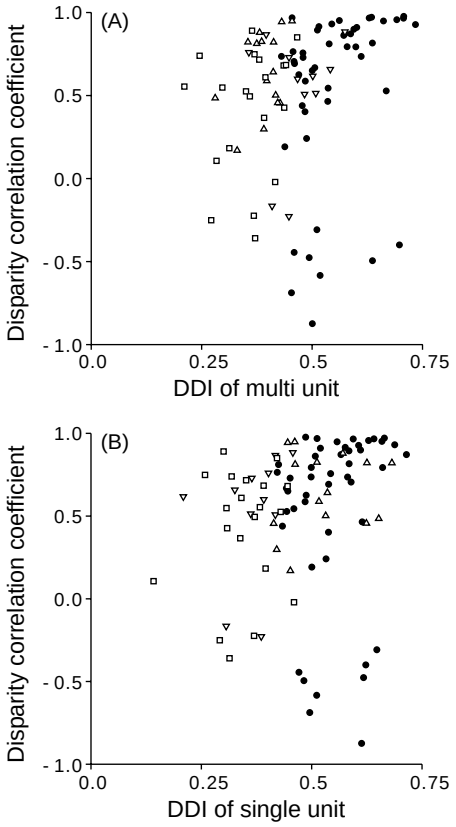

Fig. 6. Disparity correlation coefficients plotted against the disparity discrimination index (DDI) of MU (A) and SU (B). There was a weak correlation between disparity discrimination coefficients and DDI of MU ($r = 0.20$, $n = 93$; $P < 0.05$). The correlation was slightly short of statistical significance for the SU ($r = 0.17$, $n = 93$; $P = 0.057$). Symbols are as in Fig. 5.

3.3. Disparity selectivity of neurons along electrode penetrations

Given the tendency for neurons with similar disparity selectivity to cluster locally, we assessed the spatial dimension of clusters by analyzing the disparity selectivity of neurons successively encountered along electrode penetrations. In this experiment, we recorded MU responses regularly at 0.2 mm intervals, and when possible, we isolated SUs from the MU recordings. We analyzed the results from 63 electrode penetrations where recordings were made at six or more different depths and disparity-selective visual responses were obtained at least at 2 sites (21 in monkey 1, 42 in monkey 2).

Fig. 7 shows an example of an electrode penetration perpendicular to the cortical surface. The penetration was located in the posterior part of the TEd (Fig. 7A). Microscopic observation of histological sections indicates that this penetration was nearly parallel to the columnar strings of neuronal somata (Figs. 7B and 8). Along this penetration, MUs that preferred uncrossed disparities (Kruskal–Wallis test, $P < 0.05$) were recorded at four consecutive sites spanning 0.6 mm in the superficial layers (sites 1–4 in Fig. 7C).

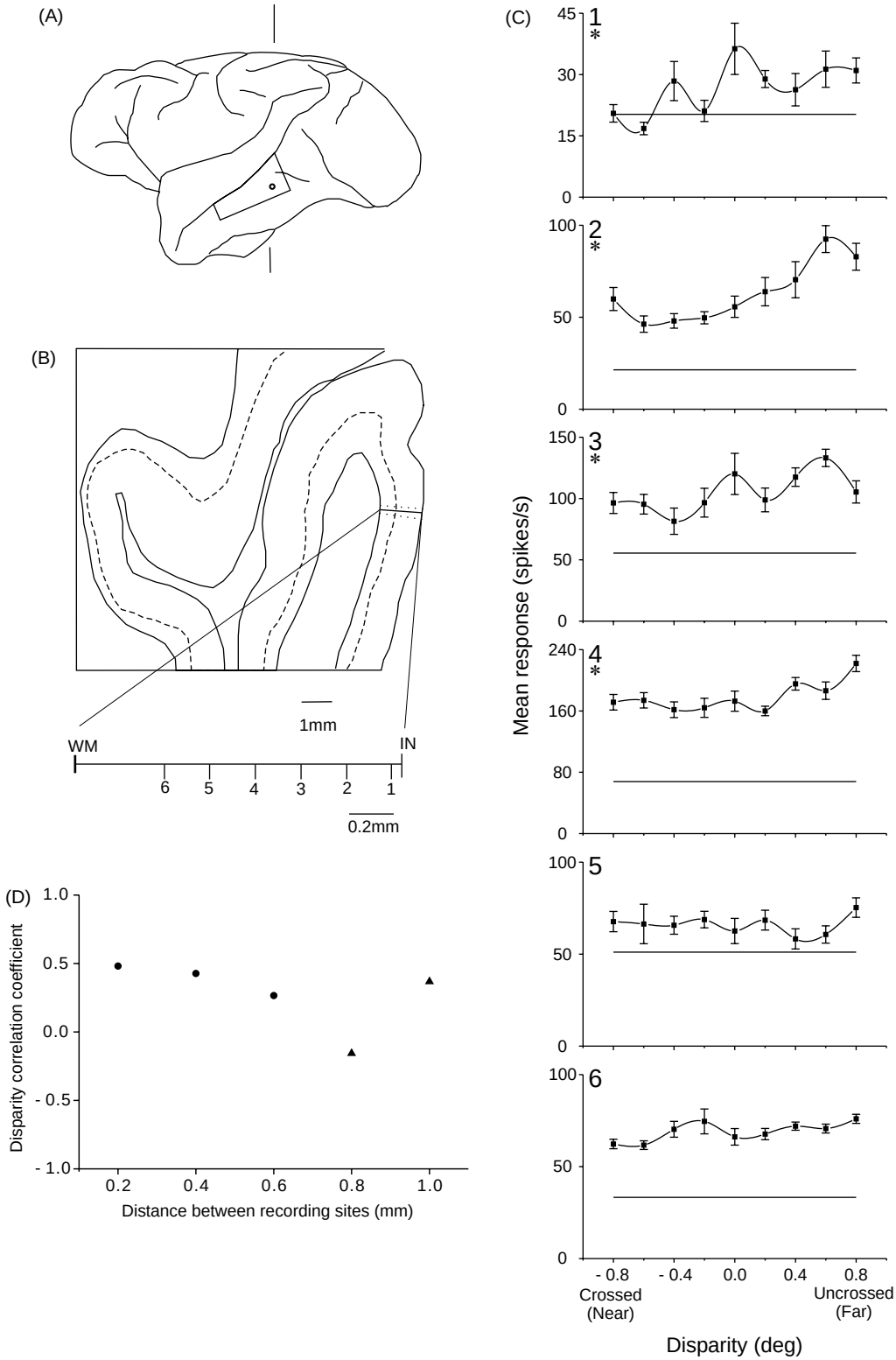

Fig. 7. Disparity–tuning curves of neurons recorded along a penetration. (A) The location of this penetration. A vertical line shows the plane at which the section was taken for (B) and Fig. 8. (B) Histological reconstruction of the electrode track. Dotted lines show the radial array of cells. The dashed line shows layer 4. Numbers 1–6: the recording sites for MUs; IN: site where the first neuron was recorded in this penetration; WM: entry into white matter. (C) The sequence of disparity tuning curves for MU1–6. Error bars indicate the standard error of the mean. Asterisks indicate disparity-selective sites (Kruskal–Wallis test, $P < 0.05$). (D) Changes in the disparity correlation coefficient between the first disparity-selective MU and the other MUs as a function of distance between sites. circles; both units were disparity selective. triangles; one of the units was disparity selective.

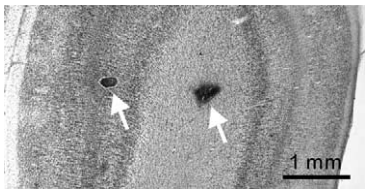

Fig. 8. Microphotograph of the histological markings (arrows) for the penetration shown in Fig. 6B.

The MUs recorded at sites 5 and 6 in deeper layers were not selective for disparity (Kruskal–Wallis test, $P > 0.05$). The disparity correlation coefficient between the MU responses recorded at site 1 and those at the other recording sites were positive and relatively high (0.27–0.48) except for the correlation between site 1 and site 5 (−0.16) (Fig. 7D). These results indicate that neurons with similar disparity selectivity were arrayed vertically in the superficial layers along this penetration.

Fig. 9 shows an example of a penetration along which far-type MU clusters and near-type MU clusters were alternately encountered. We were unable to verify this penetration histologically; however, the position of this penetration relative to other histologically recovered penetrations suggests that it was located near the tip of the posterior middle temporal sulcus at the border between the TEO and the TE (Fig. 9A). The distance between the initial recoding depth and the entry point to the white matter was as long as 3.7 mm (Fig. 9B), suggesting that this penetration traversed at a shallow angle to the cortex. The MU recorded in the middle of the third and the fourth recording sites is not shown (Fig. 9B), because responses were not evoked at this site by any of the stimuli in the set. Along this penetration, the preferred range of disparity (near or far) changed every 0.2–0.4 mm as the electrode advanced (Fig. 9C). The disparity correlation coefficient between the MU response recorded at the first disparity-selective site (site 2) and that at the other sites flipped dramatically between negative and positive values with distance (−0.82 to +0.96, Fig. 9D). The results indicate that different types of disparity-selective neurons were grouped in 0.2–0.4 mm clusters along this penetration.

We then quantitatively analyzed how the preferred disparity and disparity correlation coefficient changed with the distance between two recording sites along a penetration. We obtained 413 (150 in monkey 1, 263 in monkey 2) visually responsive MUs (Wilcoxon's signed rank test, $P < 0.05$) along the 63 penetrations. Of the 413 MUs, 269 were disparity selective (Kruskal–Wallis test, $P < 0.05$), and 192 of these 269 disparity-selective MUs had a preferred disparity within the examined range of disparity (less than ±0.8°). We examined the preferred disparity and the disparity correlation coefficient of these 192 recording sites. As we identified the penetration angles for only nine penetrations and could not assess the angles for the majority of penetrations, we pooled all the data without consideration of the angles in this analysis.

Fig. 10A shows the relationship between the preferred disparity and the distance between the recording sites. The data for 0.0 mm shows the mean absolute difference in preferred disparity (|Δ preferred disparity|) of SU and MU at the same recording site. Data points for 0.2–0.8 mm show |Δ preferred disparity| between MUs recorded at two sites separated by 0.2–0.8 mm along a penetration. |Δ preferred disparity| depended on the distance between the two recording sites (ANOVA, $P < 0.05$). |Δ preferred disparity| at 0.0 and 0.2 mm were 0.27 ± 0.07 ($n = 19$) and 0.32 ± 0.04 ($n = 76$), respectively, which were smaller than |Δ preferred disparity| calculated for randomly chosen unit pairs (0.44 ± 0.003, $n = 18336$; horizontal line in Fig. 10A; Mann–Whitney U-test, $P < 0.05$). |Δ preferred disparity| at 0.4, 0.6, and 0.8 mm were 0.45 ± 0.06 ($n = 61$), 0.49 ± 0.06 ($n = 43$), and 0.47 ± 0.07 ($n = 35$), which were not different from the value for the randomly chosen pairs ($P > 0.1$).

Fig. 10B shows the mean disparity correlation coefficient between pairs of disparity-selective sites as a function of the distance between recording sites along a penetration. The disparity correlation coefficient was dependent on the distance between two recording sites (ANOVA, $P < 0.05$). The disparity correlation coefficients at 0.0 mm distance (0.54 ± 0.13, $n = 19$) and 0.2 mm distance (0.33 ± 0.06, $n = 76$) were higher than that for two randomly chosen MUs (0.097 ± 0.003, $n = 18{,}336$, horizontal line in Fig. 10B; Mann–Whitney U-test, $P < 0.0001$). The disparity correlation coefficients at 0.4 mm (0.16 ± 0.07, $n = 61$), 0.6 mm (0.18±0.09, $n = 43$), and 0.8 mm (0.09±0.09, $n = 35$) were not different from the correlation coefficient for randomly chosen pairs (Mann–Whitney U-test, $P > 0.1$). Similar results were obtained by analyzing all 269 disparity-selective MU recording sites. The results in Fig. 10A and B suggest that, on average, clusters of neurons with similar disparity selectivity spanned more than 0.2 mm but were no larger than 0.4 mm.

One concern about the above results is the possibility that MU recordings may have sampled the same neuron at two consecutive recording sites, yielding the high correlation between them. In four penetrations, we obtained SUs at two successive recording sites, and in 1 penetration, we isolated SUs at three successive recording sites. DDIs of these SUs were 0.39–0.56 (0.49 ± 0.01, mean ± S.E., $n = 11$). The disparity correlation coefficients between neighboring sites (0.1, 0.2 or 0.4 mm apart) were 0.72–0.96 for five cases and −0.73 and −0.93 for the other two cases (median 0.78, $n = 7$). The results from SUs were thus comparable to those from MUs described above (see Fig. 6).

For comparison, we next examined how similarity of shape selectivity varied with the distance between a pair of recording sites along a penetration. We calculated Pearson's correlation coefficients for responses to the 20 stimuli in the set between two recording sites along a penetration (hereafter referred to as "shape correlation coefficient"). The analysis was performed for the same 63 penetrations used for the analysis of disparity selectivity (Fig. 10A

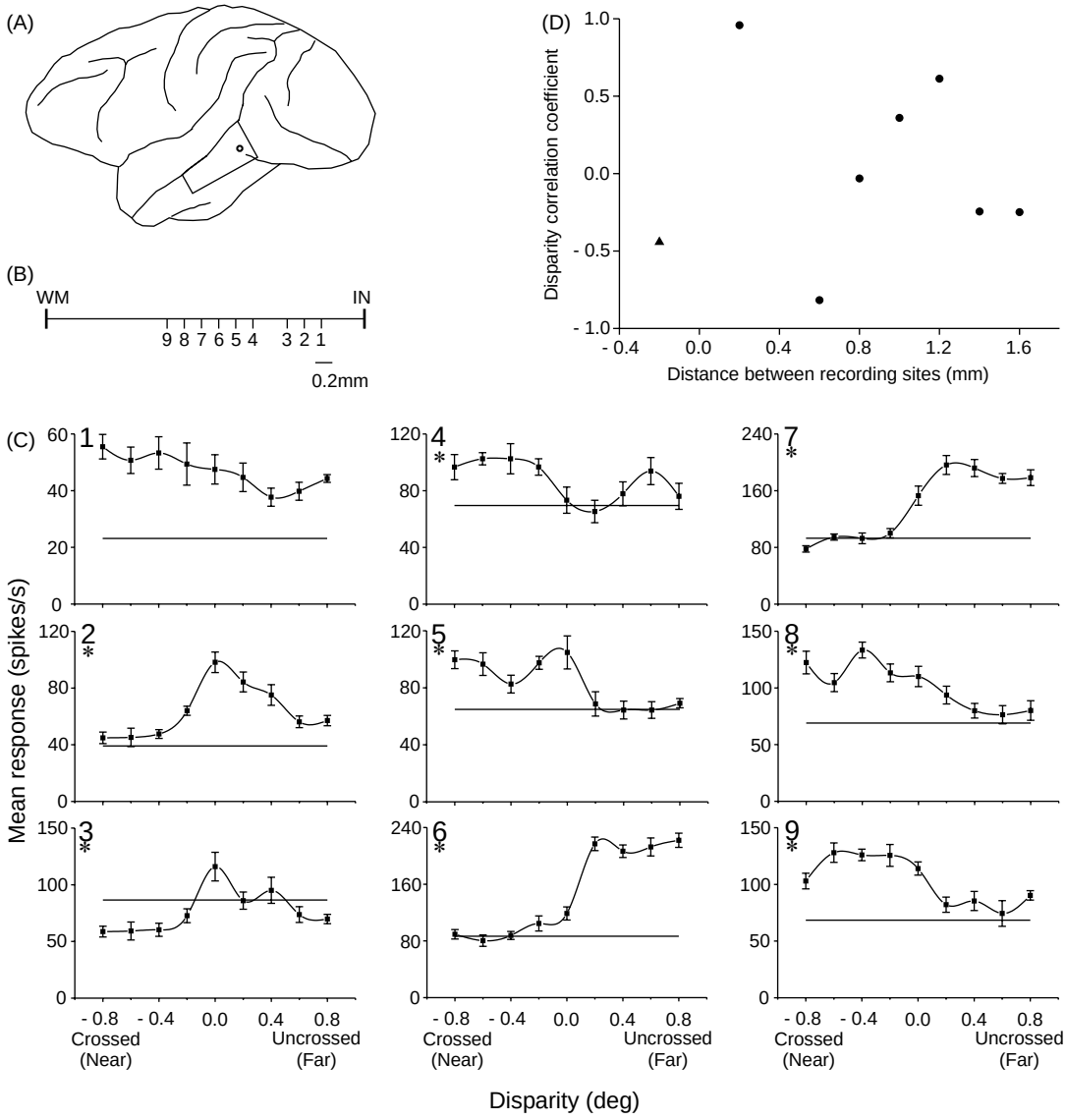

Fig. 9. Sequence of MU disparity–tuning curves recorded along a penetration. See Fig. 6 legend for conventions. Part (B) shows the schematic drawing of this recording track.

and B) where MUs at 427 sites showed shape selective responses (Kruskal–Wallis test, $P < 0.05$). Fig. 10C shows the mean shape correlation coefficient between pairs of shape-selective sites as a function of the distance between the sites along a penetration. The shape correlation coefficients statistically differed among the different distances between recording sites (ANOVA, $P < 0.0001$). The mean shape correlation coefficient was almost the same for 0.0 mm and 0.2 mm, but gradually decreased at 0.4, 0.6, and 0.8 mm. The mean shape correlation coefficient between SU and MU at the same recording site (designated as distance 0 in Fig. 10C) was 0.49 ± 0.06 ($n = 38$) and was statistically different from that for randomly chosen pairs (0.023 ± 0.001, $n = 90951$, horizontal line in Fig. 10C; Mann–Whitney U-test, $P < 0.0001$). The shape correlation coefficients from two shape-selective MUs 0.2 mm apart (0.44 ± 0.02, $n = 311$), 0.4 mm apart (0.27 ± 0.02, $n = 270$), 0.6 mm apart (0.17 ± 0.02, $n = 222$), and 0.8 mm apart (0.14 ± 0.02, $n = 184$) were all higher than that for two randomly chosen multi units (Mann–Whitney U-test, $P < 0.0001$).

4. Discussion

SU and MU responses recorded at the same site showed positive correlations in their disparity tuning curves and in their DDIs, and tended to share the preferred disparity. These results suggest that nearby neurons are similar in their selectivity for binocular disparity. Consecutive recordings at regular intervals along electrode penetrations indicate that neurons with similar disparity preference were clustered in local regions of 0.2–0.4 mm. Neurons in the

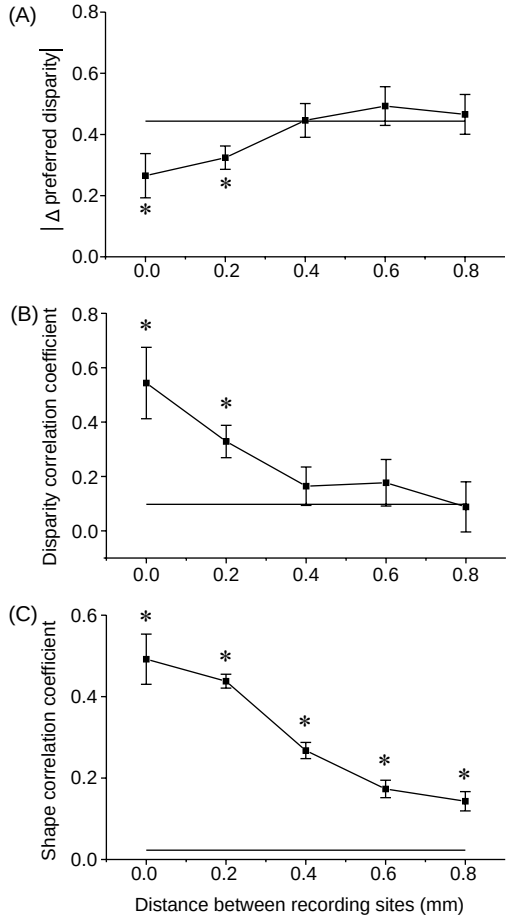

Fig. 10. (A) The absolute difference in preferred disparity (|Δ preferred disparity|) between pairs of units plotted against the distance between the units. Data were obtained from sites where both units had a peak in their disparity tuning curve within the examined range of disparity (±0.8°). Error bars indicate the standard error of the mean, and the horizontal line shows the level of each parameter for randomly drawn pairs of units from the entire population. (B) The average disparity correlation coefficient between pairs of units plotted against the distance between the units. (C) The average shape correlation coefficient between pairs of shape selective units plotted against the distance between the units. Asterisks indicate the data points statistically different from the corresponding parameters derived from two randomly chosen MUs (Mann–Whitney *U*-test, $P < 0.05$ for (A), (B) and $P < 0.0001$ for (C)).

IT are thus organized according to their disparity selectivity as well as their selectivity for object features such as shape or luminance gradation (Fujita et al., 1992; Fujita, 2002).

4.1. Separation of single units from simultaneously recorded multi units

When we compared the response of SU isolated at a site and the response of the background MU recorded at the same site, it was critically important that spikes are completely separated from each other. Otherwise, even a small amount of contamination between SU and MU would yield a false correlation in their response properties. In these experiments, we enforced precautions to avoid this potential problem in two ways. First, the windows for discriminating SU and MU were separated by an intervening gap. We ensured that even though SU showed burst firing with later spikes gradually decreasing in amplitude, these smaller spikes would not fall into the window for MU recording. Second, spikes detected with the two windows were monitored with slow and fast sweeping modes on two oscilloscopes, continuously confirming the separation between the two recording channels during experiments. In the analysis, we further showed that the high disparity correlation coefficient between SU and MU were retained for the data even when all SU spike counts were subtracted from those of the simultaneously recorded MU.

4.2. Organization of disparity-selective neurons in the IT

SU and MU responses at the same recording sites showed a higher correlation coefficient in disparity tuning curves than unit pairs recorded from different sites. Because SU and MU at the same site were recorded simultaneously and those at different sites were recorded at different times, the higher correlation for the same sites may reflect factors other than disparity selectivity. Factors influencing SU and MU responses in the same way could give rise to this correlation. These factors may include attention, fixational eye movements or changes in pupil size or accommodation. If the high correlation was due to these factors, SU–MU correlations would be independent of their disparity selectivity. However, there was a positive correlation, albeit weak, between the SU–MU correlation values and DDIs; SU–MU correlation tended to be higher for the sites with higher DDIs. These results suggest the high SU–MU correlation is a result of the architecture for binocular disparity processing. Together with the correlation of DDIs and preferred disparity between SU and MU, these results indicate that nearby neurons in the IT tend to be similar in their selectivity for binocular disparity.

There was a tendency for disparity-selective SUs to be recorded with disparity-selective MUs, and disparity-insensitive SUs to be recorded with disparity-insensitive MUs. This does not imply that the IT consists of distinct subregions of disparity-selective and disparity-insensitive neurons. Both SUs and MUs showed unimodal distributions of DDIs (Fig. 5A), indicating that IT neurons constitute a continuum of disparity selectivities rather than two discrete groups of disparity-selective and non-selective neurons. Hence, the tendency for IT neurons to cluster according to their disparity sensitivity should not be taken as evidence for the existence of discrete disparity-selective and non-selective cortical patches.

In the IT, neurons selective for similar object images or with correlated shape preferences are arrayed vertically across cortical layers in a columnar manner (Fujita et al., 1992; Wang et al., 2000; see Fujita, 2002 for review). In a penetration made almost perpendicular to the cortex, we

encountered far-neurons consecutively over 0.6 mm, but neurons in deeper layers were not selective for disparity (Fig. 7). In another penetration, far-neuron clusters and near-neuron clusters alternated every 0.2–0.4 mm (Fig. 9). On average, MUs separated by less than 0.4 mm showed similar preferred disparity and high correlation coefficients. Since we could not determine the penetration angle in most cases, we do not know whether disparity clusters were elongated in any direction. In contrast, shape correlation coefficients remained high over longer distances along penetrations (Fig. 10). Given that shape correlation coefficients rapidly fall off in tangential directions (Wang et al., 2000), we interpret this data to mean that our electrode penetrations were, in general, nearly perpendicular to the cortical surface. These results suggest that disparity neuron clusters do not extend across many cortical layers. Alternatively, if they do extend vertically to form columns, the width of similar-disparity columns is narrower than that of columns of similar shape selectivity (0.4–0.5 mm; Fujita et al., 1992; Wang et al., 1996). Further studies are required to determine whether clustering of neurons selective for similar disparities takes a columnar form in the IT and how disparity clusters relate to shape columns.

4.3. Comparison with other cortical areas

Analysis of DDIs between SU and MU has been applied to V1 (Prince et al., 2002), MT (Prince et al., 2002), and V4 (Watanabe et al., 2002). In all of these areas, the DDIs of SU positively correlate with the DDIs of MU recorded at the same site. The correlation coefficient is 0.37 for V1 (Prince et al., 2002), 0.66 for MT (Prince et al., 2002), and 0.41 for V4 (Watanabe et al., 2002). The correlation of DDIs between SU and MU for the IT was 0.54, and was thus stronger than V1 and V4, but weaker than MT. Data regarding the preferred disparity of simultaneously recorded SU and MU are also available for V1, MT, V4, and IT. Again, in all these areas, there is a significant positive correlation between the preferred disparity of SU and that of MU. The correlation is by far the strongest in MT ($r = 0.91$) compared to the other three areas ($r = 0.30$ in V1, $r = 0.43$ in V4, $r = 0.38$ in IT) (DeAngelis and Newsome, 1999; Prince et al., 2002; Watanabe et al., 2002). A common feature observed in the latter three areas is that there are sites where the preferred disparity of SU differs drastically from that of MU; e.g., one prefers crossed disparity and the other prefers uncrossed disparity. One example of this is the pair shown in the Fig. 5B inset. These results suggest that the clustering of neurons in V1, V4, and IT are weakly constrained by binocular disparity compared to the neurons in the MT. These comparisons, however, should be taken with utmost care, because the signal pickup radius of recording electrodes may differ among the studies. Even if electrodes with similar tip size and impedance are used, the effective sampling diameter may differ among different areas because the packing density of cells and the dendritic field size of pyramidal neurons differ among different cortical areas (O'kusky and Colonnier, 1982; Peters, 1987; Elston, 2002).

Acknowledgements

This work was supported by grants to I.F. from Core Research for Evolutional Science and Technology (CREST) of the Japan Science and Technology Corporation, the Ministry of Education, Culture, Science, Sports and Technology (13308046 and 15016067), and Toyota Physical and Chemical Institute. We thank Seiji Tanabe for helpful comments on this manuscript, and Masayuki Watanabe for help in data analysis. K.Y. is grateful to Professors Masatoshi Takeda and Yoshiro Sugita for their continuous encouragement during this study.

References

Adams, D.L., Zeki, S., 2001. Functional organization of macaque V3 for stereoscopic depth. J. Neurophysiol. 86, 2195–2203.
Blakemore, C., 1970. The representation of three-dimensional visual space in the cat's striate cortex. J. Physiol. (Lond.) 193, 327–342.
Burkhalter, A., Van Essen, D.C., 1986. Processing of color, form, and disparity information in visual area VP and V2 of ventral extrastriate cortex in the macaque monkey. J. Neurosci. 6, 2327–2351.
DeAngelis, G.C., Newsome, W.T., 1999. Organization of disparity-selective neurons in macaque area MT. J. Neurosci. 19, 1398–1415.
DeAngelis, G.C., Uka, T., 2003. Coding of horizontal disparity and velocity by MT neurons in the alert macaque. J. Neurophysiol. 89, 1094–1111.
Eifuku, S., Wurtz, R.H., 1999. Response to motion in extrastriate area MSTl: disparity sensitivity. J. Neurophysiol. 82, 2462–2475.
Elston, G.N., 2002. Cortical heterogeneiety: implications for visual processing and polysensory integration. J. Neurocytol. 31, 317–335.
Felleman, D.J., Van Essen, D.C., 1987. Receptive field properties of neurons in area V3 of macaque monkey extrastriate cortex. J. Neurophysiol. 57, 889–920.
Fujita, I., 2002. The inferior temporal cortex: architecture, computation, and representation. J. Neurocytol. 31, 359–371.
Fujita, I., Tanaka, K., Ito, M., Cheng, K., 1992. Columns for visual features of objects in monkey inferotemporal cortex. Nature 360, 343–346.
Hinkle, D.A., Connor, C.E., 2001. Disparity tuning in macaque area V4. NeuroReport 12, 365–369.
Hinkle, D.A., Connor, C.E., 2002. Three-dimensional orientation tuning in macaque area V4. Nat. Neurosci. 5, 665–670.
Hubel, D.H., Livingstone, M.S., 1987. Segregation of form, color, and stereopsis in primate area 18. J. Neurosci. 7, 3378–3415.
Hubel, D.H., Wiesel, T.N., 1970. Stereoscopic vision in macaque monkey. Cells sensitive to binocular depth in area 18 of the macaque monkey cortex. Nature 225, 41–42.
Janssen, P., Vogels, R., Orban, G.A., 2000. Three-dimensional shape coding in inferior temporal cortex. Neuron 27, 385–397.
Janssen, P., Vogels, R., Liu, Y., Orban, G.A., 2001. Macaque inferior temporal neurons are selective for three-dimensional boundaries and surfaces. J. Neurosci. 21, 9419–9429.
Judge, S.J., Richmond, B.J., Chu, F.C., 1980. Implantation of magnetic search coils for measurement of eye position: an improved method. Vision Res. 20, 535–538.
LeVay, S., Voigt, T., 1988. Ocular dominance and disparity coding in cat visual cortex. Vis. Neurosci. 1, 395–414.

Maunsell, J.H., Van Essen, D.C., 1983. Functional properties of neurons in middle temporal visual area of the macaque monkey. II. Binocular interactions and sensitivity to binocular disparity. J. Neurophysiol. 49, 1148–1167.

O'kusky, J., Colonnier, M., 1982. A laminar analysis of the number of neurons, glia and synapses in the visual cortex (area 17) of adult macaque monkeys. J. Comp. Neurol. 210, 278–290.

Peterhans, E., von der Heydt, R., 1993. Functional organization of area V2 in the alert macaque. Eur. J. Neurosci. 5, 509–524.

Peters, A., 1987. Number of neurons and synapses in primary visual cortex. In: Jones, E.G., Peters, A. (Eds.), Cerebral Cortex, vol. 6. Further Aspects of Cortical Function, including Hippocampus. Plenum Press, New York, pp. 267–294.

Poggio, G.F., Fischer, B., 1977. Binocular interaction and depth sensitivity in striate and prestriate cortex of behaviong monkey. J. Neurophysiol. 40, 1392–1405.

Poggio, G.F., Gonzalez, F., Krause, F., 1988. Stereoscopic mechanisms in monkey visual cortex: binocular correlation and disparity selectivity. J. Neurosci. 8, 4531–4550.

Prince, S.D.J., Pointon, A.D., Cumming, B.G., Parker, A.J., 2002. Quantitative analysis of the responses of V1 neurons to horizontal disparity in dynamic random-dot stereograms. J. Neurophysiol. 87, 191–208.

Roe, A.W., Ts'o, D.Y., 1995. Visual topography in primate V2: multiple representation across functional stripes. J. Neurosci. 15, 3689–3715.

Roy, J.P., Komatsu, H., Wurtz, R.H., 1992. Disparity sensitivity of neurons in monkey extrastriate area MST. J. Neurosci. 12, 2478–2492.

Taira, M., Tsutsui, K.I., Jiang, M., Yara, K., Sakata, H., 2000. Parietal neurons represent surface orientation from the gradient of binocular disparity. J. Neurophysiol. 83, 3140–3146.

Tanaka, H., Uka, T., Yoshiyama, K., Kato, M., Fujita, I., 2001. Processing of shape defined by disparity in monkey inferior temporal cortex. J. Neurophysiol. 85, 735–744.

Ts'o, D.Y., Roe, A.W., Gilbert, C.D., 2001. A hierarchy of the functional organization for color, form and disparity in primate visual area V2. Vision Res. 41, 1333–1349.

Uka, T., Tanaka, H., Yoshiyama, K., Kato, M., Fujita, I., 2000. Disparity selectivity of neurons in monkey inferior temporal cortex. J. Neurophysiol. 84, 120–132.

Wang, G., Tanaka, K., Tanifuji, M., 1996. Optical imaging of functional organization in the monkey inferotemporal cortex. Science 272, 1665–1668.

Wang, Y., Fujita, I., Murayama, Y., 2000. Neuronal mechanisms of selectivity for object features revealed by blocking inhibition in inferotemporal cortex. Nat. Neurosci. 3, 807–813.

Watanabe, M., Tanaka, H., Uka, T., Fujita, I., 2002. Disparity-selective neurons in area V4 of macaque monkeys. J. Neurophysiol. 87, 1960–1973.

Wheatstone, C., 1838. Contribution to the physiology of vision. Part the first. On some remarkable, and hitherto unobserved, phenomena of binocular vision. Philos. Trans. R. Soc. Lond. B. Biol. Sci. 2, 371–393.

Yoshiyama, K., Uka, T., Tanaka, H., Fujita, I., 2000. Distribution of neurons in monkey inferior temporal cortex. Neurosci. Res. Suppl. 23, S73.